RESEARCH ARTICLE

Cardo Bisphenol Fluorene Fused with Dibenzo[*g*,*p*]chrysene for a High Refractive Index Monomer

Toko Yura,[a] Rion Noda,[a] Ikuma Okada,[a] Zhenfeng Guo,[b] Takashi Nakanishi,[b] Yousuke Yamaoka,[c] and Tetsuo Iwasawa*[a]

[a] T. Yura, R. Noda, I. Okada, Prof. Dr. T. Iwasawa
Department of Materials Chemistry, Faculty of Science and Technology
Ryukoku University, Seta, Otsu, Shiga 520-2194 (Japan)
E-mail: iwasawa@rins.ryukoku.ac.jp

[b] Z. Guo, Prof. Dr. T. Nakanishi
Division of Soft Matter, Graduate School of Life Science, Hokkaido University,
Kita 10, Nishi 8, Kita-ku, Sapporo 060-0810, Japan
E-mail: NAKANISHI.Takashi@nims.go.jp
Research Center for Materials Nanoarchitectonics (MANA), National Institute for Materials Science (NIMS)
1-1 Namiki, Tsukuba 305-0044, Japan

[c] Prof. Dr. Y. Yamaoka
School of Pharmacy, Hyogo Medical University, Minatojima, Chuo-ku, Kobe, 650-8530 (Japan)

Abstract: Synthesis and properties of a new cardo-typed bis-phenol are described. A dibenzo[*g*,*p*]chrysene (DBC) core that has one ester group at the *bay* was prepared, and then intramolecular Friedel-Crafts acylation gave a key cyclopentanone intermediate. Finally, two-fold arylation successfully yielded a DBC-linked bis-phenol. This new DBC-linked bis-phenol was compared with the prototype bis-phenol fluorene (BPF). The structure-activity relationship between these two bis-phenols reveals that the expansion of the π-conjugated system using a skeletal DBC influences the quality of its attributes with a refractive index of 1.83. This comparative study provides us a basis for future cardo structure material chemistry.

Introduction

Bisphenol fluorene (BPF) is a monomer used in the production of cardo resins, which are known for their high-performance optical properties (Figure 1(a)).[1] BPF-based polymers exhibit high transparency, a high refractive index, and outstanding thermal stability, making them suitable for advanced optical applications such as lenses, optical fibers, and other components.[2,3,4] BPF monomer when polymerized leads to a cardo polymer, characterized by spiro-carbon containing pendant rings.[5] The spiro-carbon creates a point of rigidity in the molecule and suppresses inter- and intra-molecular interactions, which is a reason why BPF-based polymers show remarkable material properties in terms of refractive index, birefringence, and Abbe's number.[6,7]

There are two main approaches to improve the performance of BPF, which take a structure-activity approach: modifying the phenol moiety and altering the fluorene backbone. [1,4,8,9] While many chemical modifications have been made to the phenol moiety, there have been relatively fewer examples of altering the fluorene skeleton. [10,11] Replacing the fluorene segment with a polyaromatic hydrocarbon substructure expands the π-conjugation, which is expected to improve the material's optical properties. [12] However, this modification reduces solubility in organic solvents, making practical synthesis more challenging.

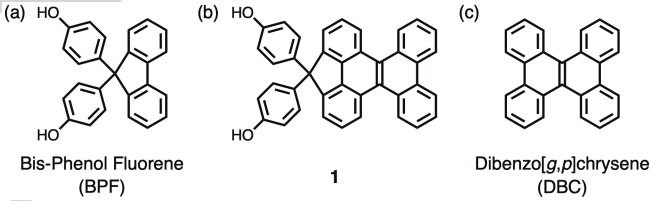

Figure 1. (a) A typical cardo structure of bis-phenol fluorene (BPF, namely 9,9-bis(4-hydroxyphenyl)fluorene, CAS RN: 3236-71-3); (b) hepta-cyclic cardo bisphenol **1**; (c) dibenzo[*g*,*p*]chrysense (DBC).

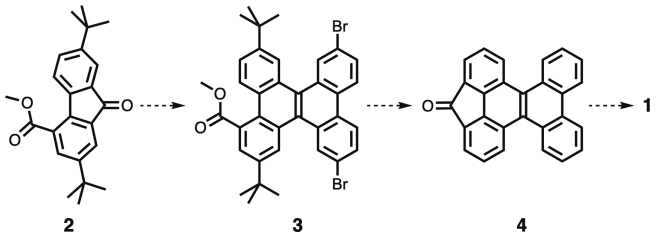

Scheme 1. Proposed scheme to synthesize cardo **1** through key intermediates of fluorenone **2**, and ester **3**, and cyclopentanone **4**.

Herein we present the synthesis of cardo bisphenol **1** in which a skeletal dibenzo[*g*,*p*]chrysene (DBC) fuses into BPF (Figure 1(b) and (c)). We anticipated that extending the π-conjugation in DBC would yield prominent BPF properties, while preserving solubility. In a recent study, our group developed a solvent-alone-driven cross-coupling to synthesize unsymmetric DBC derivatives.[13] Building on that approach, we designed a synthetic route to **1** utilizing three key precursors: fluorenone **2**, ester **3**, and cyclopentanone **4** (Scheme 1).

Results and Discussion

At the outset of our study, **2** was synthesized (Scheme 2). First, commercially available 2,7-di-*tert*-butyl-9-fluorene underwent regio-defined formylation at the 4-position in 97% yield.[14] Then, Bolm oxidation using *tert*-butyl hydroperoxide (TBHP) and $FeCl_3$ efficiently carried out two different oxidations in 92% yield.[15] Finally, methyl esterification under basic condition formed **2** surely in 74% yield. Each derivative in the sequence was additionally prepared on multi-gram scale.

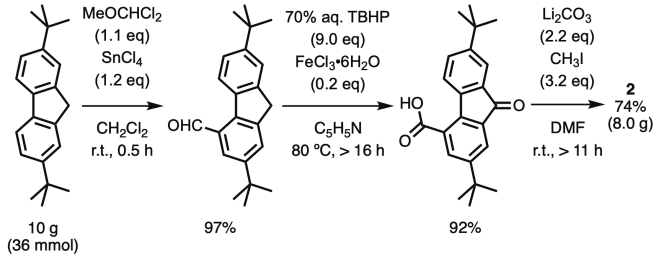

Scheme 2. Gram-scale synthesis of **2**. TBHP, *tert*-butyl hydroperoxide.

Cross-dimerization between **2** and 2,7-dibromo-9-fluroenone yielded the corresponding spiroketone **5** quantitatively (Scheme 3).[13] The ketone was subjected to reduction by $NaBH_4$, which was followed by Wagner-Meerwein rearrangement to form **3** in 93% yield. Each process was compatible with solution-phase multi-gram technique.

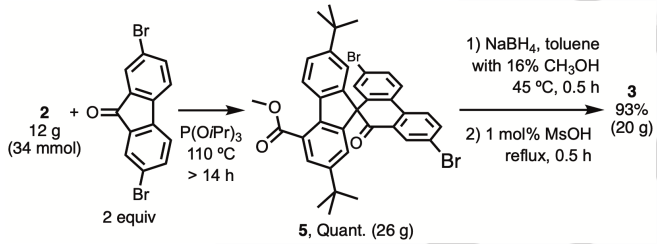

Scheme 3. Cross-dimerization between **2** and 2,7-dibromo-9-fluorenone to form **5**. The following two-step access, including reduction and migration, to DBC **3**. MsOH, methanesulfonic acid.

The hydrolysis of ester **3** yielded the corresponding carboxylic acid **6**, which was transformation into the acid chloride **7** in quantitative yield (Scheme 4). The acid chloride underwent $AlCl_3$-mediated intramolecular Friedel-Crafts acylation to yield 70% of cyclopentanone **8**.[16] Then, palladium-catalyzed dehalogenation of **8** proceeded, giving **9** in 88% yield.[17] Removal of *tert*-butyl groups of **9** produced hepta-cycle ketone **4** in 84% yield. The molecular structure of **4** was determined by crystallographic analysis, which made apparent its hepta-cycle with non-planar pi-conjugation (Figure 2).[18] The hepta-cycle constructs one bridge through the carbonyl group, and selected bond lengths and angles were depicted (part (a)). The *cove* area is expanded with the mentioned angles of about 113.86° and 115.93° presumably due to tying aryls with the carbonyl moiety. A twisted topology was also found with dihedral angle of about 30.55° that was smaller than 35.6° in unsubstituted DBC (part (b), (c) and (d)).[19] The interlayer distance in packing structure was 3.554 Å (Figure S1 in Supporting Information).

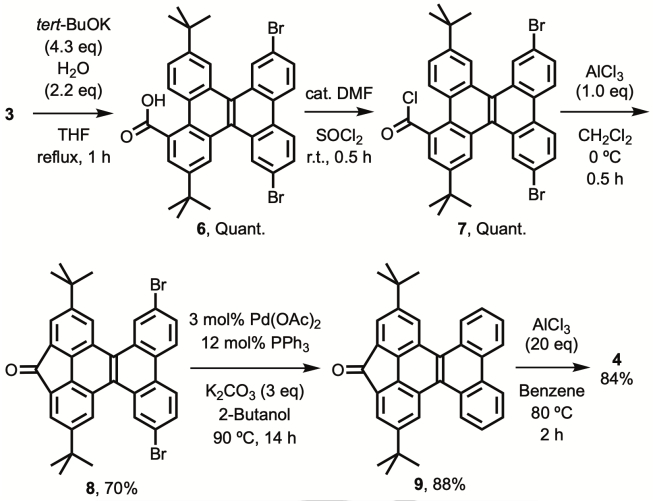

Scheme 4. Synthesis of hepta-cyclic ketone **4** through DBC derivatives **6**, **7**, **8**, and **9**.

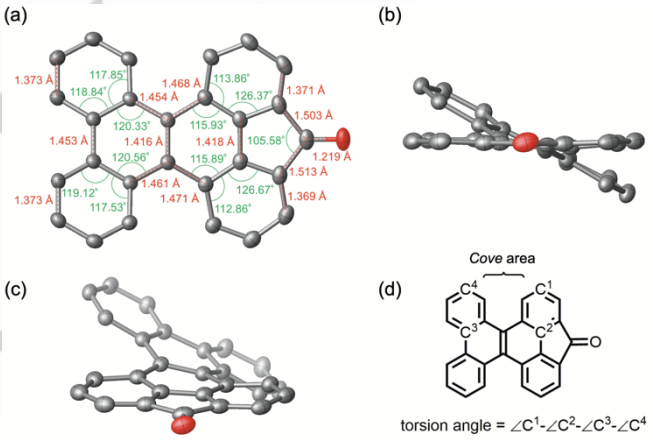

Figure 2. ORTEP drawing of **4** with thermal ellipsoids at the 50% probability level (the hydrogen atoms are omitted for clarity); (a) top view with a description of selected bond lengths and angles, (b) side-view from a ketone moiety, (c) side-view from a slanting upper part (substructure in the foreground are colored darker), (d) torsion angle, 30.55(6)°, determined by the four carbon atoms of C^1, C^2, C^3, and C^4.

With **4** in hand, direct substitution reaction through activation of the carbonyl group with methane sulfonic acid in phenol solvent was attempted. The reaction smoothly occurred, yielding **1** in 69% as white solid materials (Scheme 5). The solubility of **1** was evaluated by dissolving a 5.0 mg sample in 5.0 mL solvent. **1** dissolves well in $CHCl_3$, acetone, CH_3CN, $(CH_3)_2NCHO$, and $(CH_3)_2SO$, but remains poorly soluble in hexane, toluene, and CH_2Cl_2. In contrast, BPF is only insoluble in hexane, yet dissolves readily in all the other tested solvents.[11] The molecular structure of **1** was determined by crystallographic analysis, which made apparent its *cardo* structure (Figure 3).[20] The molecule exhibits a hepta-cycle fused ring structure (part (a)), and spreads its twofold phenol moieties wide over space (part (b)).

In addition, the hepta-cycle substructure proves to be twisted (part (c)), and the contorted shape is similar to **4**. The angle of 102.1° at the quaternary spiro-carbon of **1** narrowed as compared to that of 105.6° at the carbonyl sp^2-carbon of **4** (part (d)). The dihedral angle of **1** according to part (e) displayed 32.1(3)°, which was larger than the angle 30.55(6)° of **4**. The twisted-shape turned out to be common between **1** and **4**. Packing views of cardo **1** were also obtained (Figure 4). The hexa-cycle pi-surface tends to overlap and slant a little with each other. The pi-surfaces seem to interact with another aromatic moiety with the stacking distance of approximately 3.38 Å.

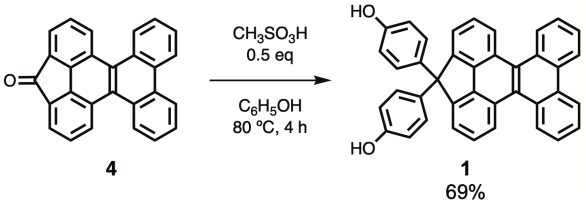

Scheme 5. Synthesis of bis-phenol **1**. MsOH: methanesulfonic acid.

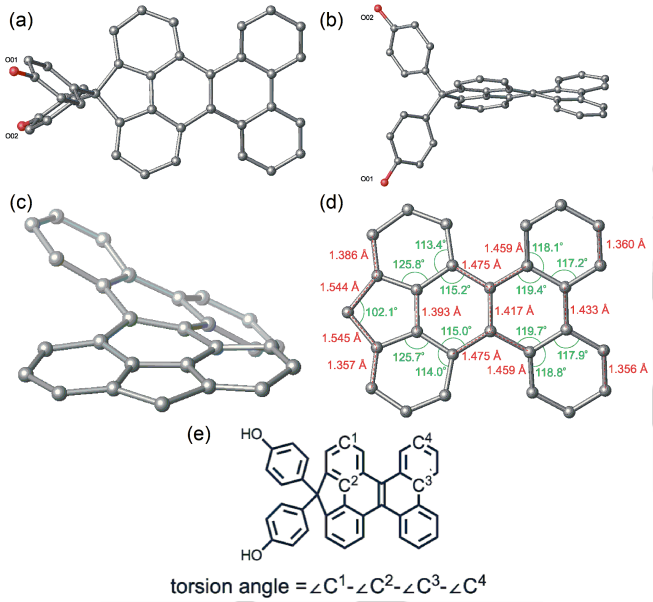

Figure 3. Molecular structures with ORTEP drawing of **1** with thermal ellipsoids at the 50% probability level (the hydrogen atoms are omitted for clarity); (a) top view, (b) side-view from a *cove* region, (c) side-view from a slanging upper part (phenol groups are removed for ease of viewing, and substructure in the foreground are colored darker), (d) top view with a description of selected bond lengths and angles, and (e) torsion angle, 32.1(3)°, determined by the four carbon atoms of C^1, C^2, C^3, and C^4.

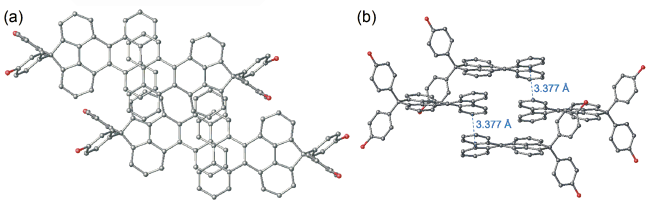

Figure 4. Molecular packing structure of **1** with ORTEP drawings with description of inter-molecular distance (3.377 Å); (a) top view, and (b) side view. The hydrogen atoms are omitted for clarity.

DFT calculations were performed to clarify information on the frontier orbitals of **1** at the B3LYP/6-31G(d,p) level of theory.[21] Structural optimization of **1** was performed using X-ray crystallography as an initial structure, wherein the optimized structure reproduced the twisted structure. Regarding the molecular orbitals, the HOMO is affected by DBC moiety although the contribution of bisphenol cardo substructure is significant in the HOMO-1 (Figure 5). For the LUMO and LUMO+1, orbitals located on DBC skeletons. In terms of energy, HOMO-LUMO gap of 3.84 eV was larger than that of an unsubstituted DBC (3.13 eV).[22]

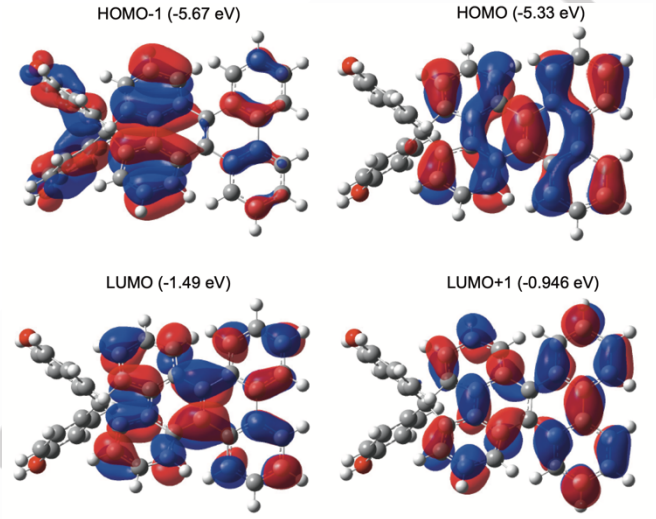

Figure 5. Frontier orbitals mappings and the energies for **1** calculated at the B3LYP/6-31G(d,p) level of theory.

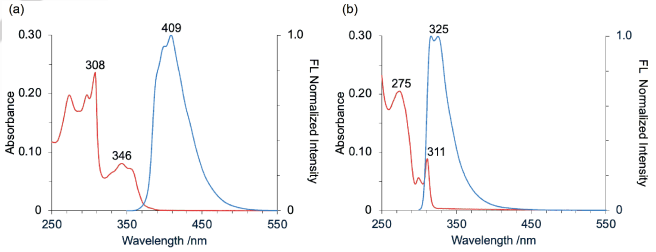

Figure 6. UV/Vis absorption (red line) and fluorescence (blue line) spectra of (a) **1**, and (b) BPF (1.0×10^{-5} M in CH_2Cl_2, excitation wavelength: 308 nm for **1** and 275 nm for BPF).

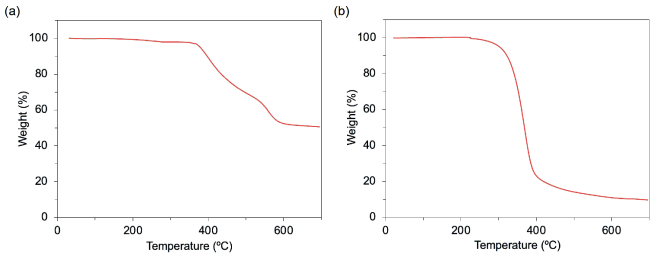

Figure 7. TGA graphs at a heating rate of 10 °C/min from ambient temperature to 700 °C under argon flow, red line for % of weight: (a) **1**, and (b) BPF. Each 5% weight loss temperature (T_{d5}) is 378 °C for **1** and 302 °C for BPF.

In order to evaluate properties of **1**, compared with the widely used BPF, the spectroscopic properties were investigated using UV/Vis absorption and photoluminescence measurements (Figure 6). **1** showed significant red shift in comparison with that of BPF, presumably due to the enlarged pi-conjugation of DBC framework. Furthermore, the solvent polarity did not noticeably affect the absorption and fluorescence spectra of **1** (Figure S3 and Table S2). As the absolute photoluminescence quantum yields were evaluated, BPF reached 19.9% and **1** provided 7.3%. For TGA values of 5% weight loss temperature (T_{d5}), **1** provided higher 378 ºC than 302 ºC of BPF (Figure 7). The observed increase in T_{d5} of **1** indicates that the rigidity inherent in its polyaromatic hexa-cycle fused-ring enhanced the thermal resistance of the bis-phenol. Refractive indices of BPF and **1** were depicted in Table 1: this study adopted a method of extrapolating the measurement results based on the concentration dependence of the dispersion solution.[23] Commercially available BPF reached 1.64,[24] while **1** achieved high 1.83. The 0.19 higher value suggests that **1** exhibits superior optical performance compared to BPF, because increasing light-bending capability makes **1** more suitable for precise optical application and device such as a plastic lens.[25]

Table 1. A comparison between **1** and BPF with respect to their optical and physical properties.

	1	BPF [a]
$\lambda_{abs,max}$	308	275
$\lambda_{ems,max}$	409	325
PLQY [%] [b]	7.3	19.9
Melting point [ºC]	> 350	224 – 226 (223 - 224) [c]
T_{d5} [ºC] [d]	378	302
Refractive index [e]	1.83	1.64 (1.68) [c]

[a] BPF purchased from TCI. [b] Absolute photoluminescence quantum yield (1.0×10^{-5} M in CH_2Cl_2). [c] The numbers in parenthesis were referred to the website of prominent supplier, see ref-[24]. [d] T_{d5} for 5% weight loss temperature, measured by thermogravimetric analysis (TGA). [e] Na-D line, 589 nm at 298 K.

Conclusion

The formation of a cardo bis-phenol moiety which resides in a bay region of DBC core, provides a new architecture for high refractive index monomer. The creation and analysis of **1** is the only one example among cardo molecules, and nothing like it has been made in synthetic chemistry so far. Three important features from this study are worthy of note. First, ketone **4** was constructed through the intra-molecular Friedel-Crafts acylation, in which the solvent-alone-driven cross-coupling between two different fluorenones played a vital role. Second, **4** was readily transformed into cardo bis-phenol **1**, and crystallographic analysis revealed the twisted topology, and DFT calculations based on the X-ray geometry disclosed important information about π-conjugation. These results were the main purpose of beginning this work. Third, a comparison of optical and chemical properties between **1** and BPF allowed us to identify a clear distinction, in which the refractive index of **1** (1.83) was much higher than those of BPF (1.64-1.68). These results emphasize the relevance of the DBC substructure to the design of new and potent cardo-based optical devices. Further development of **1** into polymer synthesis with investigation of the properties is ongoing, and the results will be reported in due course.

Experimental Section

Synthesis of 4,4'-(4*H*-benzo[*p*]indeno[7,1,2-*ghi*]chrysene-4,4-diyl)diphenol (1). Under an argon atmosphere, to a suspension of **4** (800 mg, 2.3 mmol) in phenol (1.0 mL, 23 mmol) at 80 °C (oil bath temp.) was added methanesulfonic acid (0.07 mL, 1.1 mmol). After stirred for 4 h, the reaction mixture was allowed to cool to ambient temperature, and diluted with ethyl acetate (20 mL). The mixture was washed with brine (15 mL × 3), dried over Na_2SO_4, and concentrated *in vacuo* to give 2.2 g of crude products. The resulting sample was washed with hexane (180 mL) and dried *in vacuo* (100 °C, 1 h) to give 870 mg of the target molecules as whitish brown solid materials. Purification by short-plugged silica-gel column chromatography (toluene/EtOAc, 9:1) afforded 810 mg of the desired molecules in 69% yield as whitish yellow solid materials. Further purification by recrystallization from toluene (1000 - 841 = 159 mL, 106 mL/g) gave the first prisms of 404 mg (34%) as whitish yellow solid materials. Data: *Rf* value 0.38 (toluene/EtOAc, 4:1); M.p. > 350 °C; ^{1}H NMR (400 MHz, CD_3CN) 9.03 (dd, J = 8.5, 1.7 Hz, 2H, H-15), 8.82 (dd, J = 8.5, 1.8 Hz, 2H, H-12), 8.68 (d, J = 8.2 Hz, 2H, H-1), 7.77-7.67 (m, 8H, H-2, H-3, H-13, H-14), 7.12 (dd, J = 8.7, 2.0 Hz, 4H, phenyl H-3), 6.86 (s, 2H, OH), 6.68 (dd, J = 8.7, 2.0 Hz, 4H, phenyl H-2) ppm; ^{13}C NMR (100 MHz, DMSO-d_6); 156.2 (phenyl C-1), 150.0 (phenyl C-4), 135.2 (C-12, C-2, two peaks are overlapped), 129.9 (C-13), 129.7 (C-14), 128.8 (phenyl C-3, phenyl C-5, two peaks are overlapped), 128.4 (C-3a), 128.1 (C-3a^1), 127.6 (C-1), 127.4 (C-3), 127.3 (C-15c), 125.2 (C-15), 125.0 (C-11b), 123.9 (C-15b), 122.9 (C-15a), 115.2 (phenyl C-2, phenyl C-6, two peaks are overlapped), 66.2 (C-4) ppm; MS (DART-TOFMS) *m/z*: 525 $[MH]^+$; IR (neat): 3486 (OH), 3366 (OH), 3059, 1606, 1506, 1426, 1174, 827, 718, 560 cm^{-1}; HRMS (DART-TOFMS) calcd. for $C_{39}H_{25}O_2$: 525.1855 $[MH]^+$, found: 525.1859; Anal. Calcd for $C_{39}H_{24}O_2$; C, 89.29; H, 4.61. Found: C, 89.47; H, 4.64.

Deposition Numbers 2367919 (for **4**) and 2401647 (for **1**) contain the supplementary crystallographic data for this paper. These data are provided free of charge by the joint Cambridge Crystallographic Data Centre and Fachinformationszentrum Karlsruhe, http://www.ccdc.cam.ac.uk/structures, Access Structures service.

Supporting Information Summary

Further data are available in the supplementary material of this article.

Acknowledgements

This work was supported by JSPS Grant-in-Aid for Scientific Research (C) (22K05086), and the Joint Research Center for Science and Technology of Ryukoku University, and the NIMS Joint Research Hub Program. We thank Dr. M. P. Schramm for the helpful discussions, and Dr. Toshiyuki Iwai and Dr. Takatoshi Ito at ORIST for gentle assistance in HRMS measurements. We are grateful to Prof. Dr. K. Takasu and K. Kurokawa at Kyoto University for helpful assistance of X-ray diffraction and scattering.

Keywords: Cardo structure • Dibenzo[*g*,*p*]chrysene • Refractive index • Bisphenol fluorene • Polycycles

[1] Y. Koyama, K. Nakazono, H. Hayashi, T. Takata, *Chem. Lett.* **2010**, *39*, 2-9.

[2] S. Watanabe, K. Oyaizu, *Bull. Chem. Soc. Jpn.* **2023**, *96*, 1108-1128.

[3] T. Inada, H. Masunaga, S. Kawasaki, M. Yamada, K. Kobori, K. Sakurai, *Chem. Lett.* **2005**, *34*, 524-525.

[4] B. M. Culbertson, A. Tiba, J. Sang, Y. N. Liu, *Polym. Adv. Technol.* **1999**, *10*, 275-281.

[5] K. Sakurai, M. Fuji, *Polym. J.* **2000**, *32*, 676-682.

[6] H. Saito, T. Inoue, *J. Polym. Sci., Part B* **1987**, *25*, 1629-1636.

[7] S. Setayesh, A.C. Grimsdale, T. Weil, V. Enkelmann, K. Mullen, F. Meghdadi, E. J. W. List, G. Leising, *J. Am. Chem. Soc.* **2001**, *123*, 946-953.

[8] K. Nakabayashi, T. Imai, M.-C. Fu, S. Ando, T. Higashihara, M. Ueda, *Macromolecules*, **2016**, *49*, 5849-5856.

[9] S. Seesukphronrarak, S. Kawasaki, K. Kobori, T. Takata, *J. Polym. Sci., Part A: Polym. Chem.* **2008**, *46*, 2549-2556.

[10] H. Okuda, Y. Koyama, T. Kojima, T. Takata, *J. Polym. Sci., Part A: Polym. Chem.* **2013**, *51*, 4541-4549.

[11] S. Seesukphronrarak, S. Kawasaki, S. Kuwata, T. Takata, *J. Polym. Sci., Part A: Polym. Chem.* **2019**, *57*, 2602-2605.

[12] a) T. Takada, S. Seesukphronrarak, S. Miyauchi, M. Yamada, S. Kawasaki, Jpn. Kokai Tokkyo Koho 2009-057322, 2009; b) T. Takada, S. Miyauchi, M. Yamada, S. Kawasaki, Jpn. Kokai Tokkyo Koho 2009-057323, 2009.

[13] N. Yoshida, R. Akasaka, Y. Yamaoka, T. Yashima, Y. Tokunaga, T. Iwasawa, *Tetrahedron* **2023**, *143*, 133549.

[14] U. Grieser, K. Hafner, *Chem. Ber.* **1994**, *127*, 2307-2314.

[15] M. Nakanishi, C. Bolm, *Adv. Synth. Catal.*, **2007**, *349,* 861-864.

[16] a) N. Yoshida, R. Akasaka, T. Imai, M. P. Schramm, Y. Yamaoka, T. Amaya, T. Iwasawa, *Eur. J. Org. Chem.* **2023**, *26*, e202300407; b) N. Hamaguchi, T. Kubota, M. Yamada, H. Kimura, H. Tsuji, *Chem. Eur. J.* **2024**, *30*, e202400987.

[17] J. Chen, Y. Zhang, L. Yang, X. Zhang, J. Liu, L. Li, H. Zhang, *Tetrahedron* **2007**, *63*, 4266-4270.

[18] The single crystal of **4** was prepared by slow evaporation of CH_2Cl_2/CH_3OH (1.0 mL/4.0 mL) solution of the sample (3 mg); CCDC-2367919. Orthorhombic, space group Pbca, colorless, a = 17.4111 (8) Å, b = 9.0710 (3) Å, c = 20.9628 (6) Å, α = 90°, β = 90°, γ = 90°, V = 3310.8 (2) Å^3, Z = 8, T = 93 K, $d_{calcd.}$ = 1.422 g cm^{-3}, μ(Mo-$K\alpha$) = 0.662 mm^{-1}, R_1 = 0.0408, wR_2 = 0.1127, GOF = 1.041, Torsion angles = ∠C1-C2-C3-C4 = 30.55(6)°.

[19] Y. Ueda, H. Tsuji, H. Tanaka, E. Nakamura, *Chem. Asia. J.* **2014**, *9*, 1623-1628.

[20] The single crystal of **1** was prepared by slow evaporation of CH_2Cl_2/Hexane (2.0 mL/4.0 mL) solution of the sample (3 mg); CCDC-2401647. In compound **1**, electron density resulting from one disordered solvent molecule was removed using OLEX solvent mask. Triclinic, space group P -1, colorless, a = 9.0201 (7) Å, b = 11.4729 (10) Å, c = 16.3220 (9) Å, α = 82.369 (6)°, β = 89.010 (5)°, γ = 74.991 (7)°, V = 1616.8 (2) Å^3, Z = 2, T = 93 K, $d_{calcd.}$ = 1.252 g cm^{-3}, μ(Mo-$K\alpha$) = 2.066 mm^{-1}, R_1 = 0.0925, wR_2 = 0.2914, GOF = 1.084, Torsion angles = ∠C1-C2-C3-C4 = 32.1(3)°.

[21] Density functional theory (DFT) calculations were performed at B3LYP/6-31G(d,p) using the Gaussian 09 (Revision E.01), M. J. Frisch, G. W. Trucks, H. B. Schlegel, G. E. Scuseria, M. A. Robb, J. R. Cheeseman, G. Scalmani, V. Barone, B. Mennucci, G. A. Petersson, H. Nakatsuji, M. Caricato, X. Li, H. P. Hratchian, A. F. Izmaylov, J. Bloino, G. Zheng, J. L. Sonnenberg, M. Hada, M. Ehara, K. Toyota, R. Fukuda, J. Hasegawa, M. Ishida, T. Nakajima, Y. Honda, O. Kitao, H. Nakai, T. Vreven, J. A. Montgomery, Jr., J. E. Peralta, F. Ogliaro, M. Bearpark, J. J. Heyd, E. Brothers, K. N. Kudin, V. N. Staroverov, T. Keith, R. Kobayashi, J. Normand, K. Raghavachari, A. Rendell, J. C. Burant, S. S. Iyengar, J. Tomasi, M. Cossi, N. Rega, J. M. Millam, M. Klene, J. E. Knox, J. B. Cross, V. Bakken, C. Adamo, J. Jaramillo, R. Gomperts, R. E. Stratmann, O. Yazyev, A. J. Austin, R. Cammi, C. Pomelli, J. W. Ochterski, R. L. Martin, K. Morokuma, V. G. Zakrzewski, G. A. Voth, P. Salvador, J. J. Dannenberg, S. Dapprich, A. D. Daniels, Ö. Farkas, J. B. Foresman, J. V. Ortiz, J. Cioslowski, D. J. Fox, Gaussian, Inc., Wallingford CT, 2013.

[22] See, ref [19]: E_{HOMO} = -5.70 eV, determined by CV. E_{LUMO} = -2.57 eV, determined by optical band gap.

[23] a) J. H. Park, S. B. Kim, *Polymers* **2021**, *13*, 2907-2923; b) T. Song, G. Li, Z. Wang, M. Guo, M. Li, *Macromolecules* **2020**, *53*, 9159-9168; c) H. Park, H. Kwak, S.-Y. Jang**,** *Macromolecules* **2021**, *54*, 3586–3594; d) S. Wu, F. Li, M. Sun, Z. Wang, L. Gao, Y. Zhao, F. Bai, *Polymer* **2020**, *186*, 122034.

[24] BPF was purchased from Tokyo Chemical Industry Co., Ltd. (TCI). The website of Osaka Gas Chemicals CO., Ltd. (OGC), a prominent supplier, refers to the refractive index of 1.68 and melting point of 223-224 ºC, see: https://www.ogc.co.jp/products/fluorene/monomer.html.

[25] For example, K. You, M. Koike, Y. Suzuki, K. Sakurai, T. Indo, K. Igarashi, US Patent 6, 255, 031 (2001).

Entry for the Table of Contents

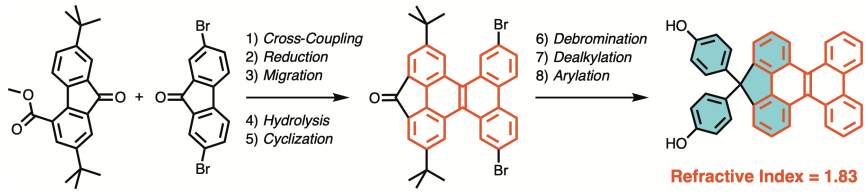

Synthesis of an unexplored cardo-typed optical material showing a high refractive index of 1.83 is described. The hepta-cycle precursor wherein dibenzo[*g*,*p*]chrysene and cyclopentanone are fused together undertook double arylation to form a quaternary carbon. The resulting cardo scaffold was ranked with the primal cardo-monomer bis-phenol fluorene in chemical properties, which clarified the efficacy of dibenzo[*g*,*p*]chrysene.

Institute and/or researcher Twitter usernames: @Ryu__iwaken